Non-Hermitian skin effect in a one-dimensional interacting Bose gas

Liang Mao [📷],[1] Yajiang Hao [📷],[2] and Lei Pan [📷][3,*]

[1]*Institute for Advanced Study, Tsinghua University, Beijing 100084, China*
[2]*Department of Physics, University of Science and Technology Beijing, Beijing 100083, China*
[3]*School of Physics, Nankai University, Tianjin 300071, China*

Non-Hermitian skin effect (NHSE) is a unique feature studied extensively in noninteracting non-Hermitian systems. In this paper, we extend the NHSE originally discovered in noninteracting systems to interacting many-body systems by investigating an exactly solvable non-Hermitian model, i.e., the prototypical Lieb-Liniger Bose gas with imaginary vector potential. We show that this non-Hermitian many-body model can also be exactly solved through the Bethe ansatz. By solving the Bethe ansatz equations accurately, the explicit eigenfunction is obtained, and the model's density profiles and momentum distributions are calculated to characterize the NHSE quantitatively. We find that the NHSE is gradually suppressed on the repulsive side but does not vanish as the repulsive interaction strength increases. On the attractive side, the NHSE for bound-state solutions is enhanced as interaction strength grows. In contrast, for the scattering state the NHSE shows a nonmonotonic behavior in the attractive side. Our paper provides an example of the NHSE in exactly solvable many-body systems, and we envision that it can be extended to other non-Hermitian many-body systems, especially to integrable models.

I. INTRODUCTION

Open quantum systems are ubiquitous in nature, and their study is an essential branch of modern physics that has penetrated into numerous areas, including atomic and molecule physics, nuclear physics, photonics, biophysics, mesoscopic physics, etc. Non-Hermitian Hamiltonians can describe an open quantum system effectively. The first example was introduced by Gamow, who derived a non-Hermitian model to describe the alpha decay of heavy nuclei [1]. With the discovery of $\mathcal{PT}$ symmetry [2] in non-Hermitian Hamiltonians and associated experimental observation of $\mathcal{PT}$-symmetry breaking, non-Hermitian physics has attracted intense attention.

In recent years, non-Hermitian physics has roused revived theoretical interest due to tremendous advances in experimental technology for controlling dissipation [3,4]. Thanks to the great advantage in manipulating atom-atom interaction and light-matter coupling, ultracold atom experiments provide an unprecedented opportunity to investigate interacting non-Hermitian systems [5–15]. Recent theoretical studies in non-Hermitian many-body systems have revealed that the interplay between interaction and non-Hermiticity can alter physical properties and give rise to intriguing phenomena absent in Hermitian many-body systems [16–71] such as non-Hermitian superfluidity [21–23], non-Hermitian quantum magnetism [42,55], and non-Hermitian many-body localization [56–58].

A unique feature of non-Hermitian systems in open boundary conditions (OBC) is the so-called non-Hermitian skin effect (NHSE) [72–76] which is recognized by eigenfunctions

accumulated at a boundary, akin to the charge distribution over the surface in a conductor. More recently, non-Hermitian systems featuring the NHSE have been raising an increasing concern [77–98] motivated by the experimental realization of NHSE [99–107]. Despite extensive investigations, the current studies of the NHSE discussed in the literature mainly focus on the single-particle level, such as non-Hermitian topological bands or non-Hermitian quasicrystals. In contrast, the research on NHSE in interacting systems is in its infancy [108–113], and just involves few-body calculation [108], exact diagonalization study [109–111], perturbation theory [112], and the hard-core limit [113]. The NHSE in exactly solvable many-body systems has not been systematically investigated so far.

In this paper, we theoretically investigate NHSE in an exactly solvable model. Exactly solvable models play a significant role in statistical physics and condensed-matter physics, such as the verification of Bogoliubov theory in the Lieb-Liniger model [114] and Wilson's numerical renormalization group in exact solutions of the Kondo model [115]. In recent years, starting from Ref. [116], there has been an increasing amount of literature on integrable open quantum systems in the framework of the Lindblad equation [117–125]. With the help of techniques developed in the integrable model literature, we can obtain exact solutions of eigenenergies and wave functions. The NHSE sensitively depends on boundary conditions, which is similar to integrability conditions in many-body systems. So we need to consider a non-Hermitian interacting system with OBC, which manifests the NHSE and meanwhile guarantees the integrability condition. Based on this criterion, we employ the one-dimensional (1D) interacting Bose gas (Lieb-Liniger model) under OBC with an additional imaginary potential corresponding to the

*panlei@nankai.edu.cn

nonreciprocal hopping in the 1D lattice [see (1)]. This model has different physical properties as interaction strength varies, and can form bound states on the attractive interaction side. We will investigate NHSE and its response to interaction in the whole interaction range.

The rest of this paper is organized as follows. In Sec. II, we introduce the exactly solvable non-Hermitian many-body model and give the exact solution obtained by the Bethe ansatz, where the explicit eigenfunction and eigenvalue are derived. In Sec. III, we discuss the NHSE in a repulsive interaction regime where both density profiles and momentum distributions are calculated to quantify the degree of the NHSE. Then we explore the NHSE in attractive interaction, including the bound state and scattering state, in Sec. IV. Finally, we summarize this paper in Sec. V. For readers who are not familiar with NHSE, Appendix A provides an introductory example for NHSE in a tight-binding model.

II. MODEL AND SOLUTION

In this section, we introduce an exactly solvable non-Hermitian many-body model and then carry out the Bethe ansatz solution. We focus on a 1D system with length L that consists of N bosons with δ-function interaction and subject to an imaginary potential:

$$\hat{H} = \sum_{j=1}^{N} \left[-i\frac{\partial}{\partial x_j} + i\phi(x_j) \right]^2 + 2c \sum_{j<l} \delta(x_j - x_l), \quad (1)$$

where c denotes the interaction strength and $i\phi(x)$ is the imaginary potential. Here we set $\hbar = 2m = 1$. This model is known as the Lieb-Liniger model [114] when $\phi(x) = 0$ and has been realized in ultracold atomic gases [126–128]. The confinement-induced resonance [129] or Feshbach resonance [130] can tune the interaction strength. The imaginary potential is related to the local loss rate, which could be realized via dissipative Aharonov-Bohm ring [131]. The detailed explanation about the relationship between local loss rate and imaginary potential is discussed in Appendix B. The Lieb-Liniger model with atom losses has been extensively investigated via Bethe ansatz in the past [132–137]. In the following we will show that the non-Hermitian model (1) can also be solved exactly both in periodic boundary condition (PBC) and OBC for uniform potential $\phi(x) = \phi$.

We start from the Schrödinger equation $\hat{H}\Psi(x_1, \ldots, x_N) = E\Psi(x_1, \ldots, x_N)$ and then we write the many-body wave function $\Psi(x_1, \ldots, x_N)$ in the following form:

$$\Psi(x_1, \ldots, x_N) = \sum_{\mathbf{P}} \psi(x_{p_1}, x_{p_2}, \ldots, x_{p_N})$$
$$\times \Theta(x_{p_1} \leqslant x_{p_2} \cdots \leqslant x_{p_N}) \quad (2)$$

where $p_1, p_2, \ldots, p_N$ presents the one of permutations of the set $1, \ldots, N$, and $\sum_{\mathbf{P}}$ is the summation of all permutations. $\Theta(x_{p_1} \leqslant \cdots \leqslant x_{p_N}) = \theta(x_{p_N} - x_{p_{N-1}}) \cdots \theta(x_{p_2} - x_{p_1})$ where $\theta(x - y)$ is the step function. Since the wave function is symmetric under the interchange of coordinates, one just needs to calculate $\psi(x_1, x_2, \ldots, x_N)$ in any region $x_1 \leqslant x_2 \leqslant \cdots \leqslant x_N$,

which satisfies

$$\left(\sum_{j=1}^{N} \left[-i\frac{\partial}{\partial x_j} + i\phi \right]^2 + 2c \sum_{i<j} \delta(x_i - x_j) \right) \psi(x_1, \ldots, x_N)$$
$$= E\psi(x_1, \ldots, x_N). \quad (3)$$

The δ-function interaction gives rise to the contact condition:

$$\left(\frac{\partial}{\partial x_{j+1}} - \frac{\partial}{\partial x_j} \right) \psi\left(\cdots x_j, x_{j+1} \cdots \right)\big|_{x_{j+1}=x_j}$$
$$= c\psi\left(\cdots x_j, x_{j+1} \cdots \right)\big|_{x_{j+1}=x_j}. \quad (4)$$

We first consider the PBC, i.e.,

$$\psi(x, x_2, \ldots, x_N) = \psi(x_1, x_2, \ldots, x + L), \quad (5)$$

with system size L. According to the Bethe ansatz solutions, the wave function takes linear superposition of plane waves:

$$\psi(x_1, x_2, \ldots, x_N) = \sum_{\mathbf{P}} A_{\mathbf{P}} \exp\left(\sum_{j=1}^{N} ik_{p_j} x_j \right), \quad (6)$$

where k_j's denote the quasimomentum of bosons. Combining the wave function (6) into contact condition (4) and boundary condition (5), quasimomenta satisfy the Bethe ansatz equations (BAEs)

$$\exp(ik_j L) = \prod_{l=1(\neq j)}^{N} \frac{ik_j - ik_l - c}{ik_j - ik_l + c}, \quad (7)$$

and the eigenenergy is given by $E = \sum_{j=1}^{N}(k_j + i\phi)^2$. The solution of quasimomenta and the corresponding eigenfunction are independent of ϕ, but the spectrum is complex, which is similar to the single-particle model in PBC as discussed in Appendix A.

We then turn to the OBC:

$$\psi(0, x_2, \ldots, x_N) = \psi(x_1, x_2, \ldots, L) = 0. \quad (8)$$

It has been shown that the Lieb-Liniger model ($\phi = 0$) in OBC can also be exactly solved [138–141]. We will show that the non-Hermitian case can be solved exactly. To solve the non-Hermitian model in OBC, we require the non-Bloch wave function obtained from the single-particle model in OBC. And then we can construct the many-body wave function by means of Bethe ansatz form

$$\psi(x_1, x_2, \ldots, x_N) = \sum_{\mathbf{P}, r_1, \ldots, r_N} A_{\mathbf{P}} \exp\left(\sum_{j=1}^{N} (ir_j k_{p_j} x_j + \phi x_j) \right), \quad (9)$$

where $r_j = 1$ ($r_j = -1$) indicates the plane wave of the jth boson moving toward right or left. We emphasis that Bethe ansatz wave function (9) is the superposition of non-Bloch wave functions instead of plane waves. The traditional ansatz for Hermitian systems in OBC, i.e., $\psi(x_1, x_2, \ldots, x_N) = \sum_{\mathbf{P}, r_1, \ldots, r_N} A_{\mathbf{P}} \exp\left(\sum_{j=1}^{N} ir_j k_{p_j} x_j \right)$, cannot solve the non-Hermitian Hamiltonian (1). Based on the wave function (9) together with Eqs. (8) and (4), one can derive the BAEs in

OBC:

$$\exp(i2k_jL) = \prod_{l=1(\neq j)}^{N} \frac{ik_j - ik_l - c}{ik_j - ik_l + c} \frac{ik_j + ik_l - c}{ik_j + ik_l + c}, \quad (10)$$

and the energy eigenvalue is given by $E = \sum_{j=1}^{N} k_j^2$. Physically, the second fraction on the right-hand side of Eq. (10) comes from the reflection at boundaries.

It is worth noting that the eigenfunction in the OBC case is related to the one of the Hermitian counterpart ($\phi = 0$) of Hamiltonian (1) by a transformation $k_j \rightarrow k_j + i\phi$. The energies and BAEs are determined simply by the Hermitian counterpart and independent on ϕ. This transformation of wave functions should manifest itself in more complicated cases with imaginary potential or nonreciprocal hopping because its validity is always guaranteed by OBC. In contrast, the wave function of the PBC case is exactly the same as the one in the Hermitian case which is independent of ϕ, but the energies depend on ϕ. The invariability of the wave function of the PBC case is closely related to the particular $k_i - k_j$ structure in BAEs which leads to the invariance of solutions under the transformation $k_j \rightarrow k_j + i\phi$.

From the above calculation, the many-body eigenfunction in OBC exhibits NHSE in the entire area of interaction $c \in (-\infty, \infty)$. The following sections will elaborate on the properties of NHSE in distinct interaction regions, including repulsive and attractive interactions.

III. NHSE IN REPULSIVE INTERACTION

In this section, we study the NHSE in repulsive interaction. When $c > 0$, the system is in a scattering state, and the solution of quasimomenta is real and unique. To analyze the solutions of BAEs, we first take the logarithm of Eq. (10) that leads to

$$k_jL = \pi I_j + \sum_{l=1(\neq j)}^{N} \left(\arctan \frac{c}{k_j - k_l} + \arctan \frac{c}{k_j + k_l} \right), \quad (11)$$

where $\{I_j\}$ represents the quantum number that takes a set of integers. For the ground state, we have $I_j = 1 \, (1 \leqslant j \leqslant N)$ which can be found in the noninteracting limit where all bosons condense on $k_j = \pi/L$. For a fixed $\{n_j\}$, one can solve Eq. (11) to determine quasimomenta for arbitrary interaction strength.

After some calculations, we can derive the explicit expression of the eigenfunction as

$$\psi(x_1, x_2, \ldots, x_N)$$

$$= \sum_{\mathbf{P}} A_{\mathbf{P}} \epsilon_{\mathbf{P}} \exp \left[i \left(\sum_{l<j}^{N-1} \Omega_{p_j p_l} \right) \right]$$

$$\times \sin(k_{p_1} x_1) \exp(ik_{p_N} L) \prod_{j=1}^{N} \exp(\phi x_j)$$

$$\times \prod_{1<j<N} \sin \left(k_{p_j} x_j - \sum_{l<j} \Omega_{p_l p_j} \right) \sin[k_{p_N}(L - x_N)], \quad (12)$$
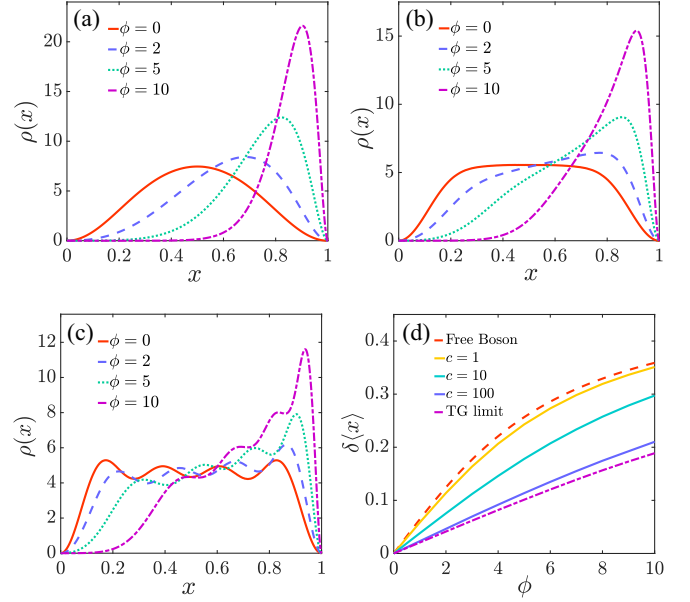

FIG. 1. NHSE in repulsive interacting bosons. Ground-state density distributions $\rho(x)$ in real space for different ϕ at (a) $c = 1$, (b) $c = 10$, and (c) $c = 100$. (d) The deviation of mean position $\delta\langle x \rangle$ as a function of ϕ for different interaction strengths from noninteracting (dashed line) to TG limit (dot-dashed line). ϕ and c are in units of $1/L$. Here we choose $L = 1$ as length unit and set $N = 4$.

where $A_{\mathbf{P}} = \prod_{j<l}^{N} (ik_{p_j} - ik_{p_l} - c)(ik_{p_j} + ik_{p_l} - c)$ and $\Omega_{jl} = \arctan \frac{c}{k_j + k_l} - \arctan \frac{c}{k_j - k_l}$. Here the sign factor $\epsilon_{\mathbf{p}}$ takes $+1$ (-1) relying on even (odd) permutations of $(p_1, p_2, \ldots, p_N)$. Apparently, the wave function meets boundary conditions (8). Thus, the eigenenergy and wave function can be determined immediately once the BAEs are solved.

To investigate the NHSE, we calculate the density distribution in real space:

$$\rho(x) = \frac{N \int_0^L dx_2 \cdots dx_N |\Psi(x, x_2, \ldots, x_N)|^2}{\int_0^L dx_1 \cdots dx_N |\Psi(x_1, x_2, \ldots, x_N)|^2}. \quad (13)$$

In Fig. 1, we plot density distributions for distinct potential ϕ at weak ($c = 1$), mediate ($c = 10$), and strong interaction ($c = 100$). Notably, the density distribution gradually tends to the right boundary with the increasing of ϕ. Meanwhile, the repulsive interaction widens the density profile. In order to characterize the degree of NHSE qualitatively, we define the deviation of mean position similar to the charge distribution:

$$\delta\langle x \rangle = \frac{1}{N} \int_0^L x[\rho(x) - \rho_0(x)]dx, \quad (14)$$

where $\rho_0(x)$ denotes the density distribution at $\phi = 0$. The larger $\delta\langle x \rangle$ is, the stronger the degree of the NHSE will be. One can see from Fig. 1(d) that the NHSE is suppressed as the interaction strength grows. It is physically reasonable that the repulsive interaction prevents bosons from clumping together, thereby effectively suppressing NHSE. However, the NHSE always exists even in the Tonks-Girardeau (TG) limit $c = \infty$. In the TG limit, the ground-state solution of the BAEs (11) is $k_j = j\pi$ $(j = 1, 2, \ldots, N)$ where the bosons look like free spinless fermions, and the corresponding wave function
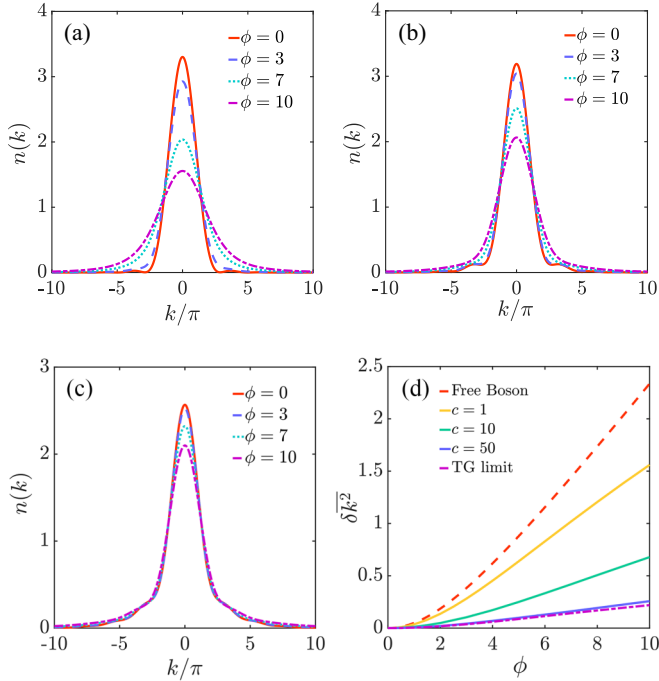
FIG. 2. Ground-state momentum distributions $n(k)$ for different ϕ at (a) $c = 1$, (b) $c = 10$, and (c) $c = 50$. (d) The deviation of momentum distribution $\delta\langle x \rangle$ as a function of ϕ for different interaction strengths from noninteracting (dashed line) to TG limit (dot-dashed line). ϕ and c are in units of $1/L$. Here we choose $L = 1$ as length unit and set $N = 4$.

takes the form of

$$\Psi(x_1, x_2, \ldots, x_N) = \sum_{\mathbf{P}} \theta(x_{p_N} - x_{p_{N-1}}) \cdots \theta(x_{p_2} - x_{p_1})$$
$$\times \prod_{j=1}^{N} \sin(j\pi x_{p_j}/L) \exp(\phi x_{p_j}), \quad (15)$$

which leads to finite $\delta\langle x \rangle$ as shown in Fig. 1(d).

We can also characterize the magnitude of NHSE via momentum distribution $n(k) = \frac{1}{2\pi} \int_0^L dx \int_0^L dx' \varrho(x, x') e^{-ik(x-x')}$ where the single-particle density matrix $\varrho(x, x')$ is defined as

$$\varrho(x, x')$$
$$= \frac{N \int_0^L dx_2 \cdots dx_N \Psi^*(x, x_2, \ldots, x_N) \Psi(x', x_2, \ldots, x_N)}{\int_0^L dx_1 dx_2 \cdots dx_N |\Psi(x_1, x_2, \ldots, x_N)|^2}.$$
$$(16)$$

The momentum distribution width is enhanced as ϕ increases, as shown in Figs. 2(a)–2(c). The broadening momentum distribution corresponds to the NHSE in real space, where particles concentrate on the boundary with a narrower density profile according to the Fourier transformation. Specifically, Fig. 2(d) plots the deviation of momentum distribution width $\delta\overline{k^2} = \overline{k^2} - \overline{k^2}_{\phi=0}$ with $\overline{k^2} = \int_{-\infty}^{\infty} k^2 n(k) dk$ as a function of ϕ at different interaction strengths where the suppression of the momentum distribution width growth by repulsive interaction can be visualized.
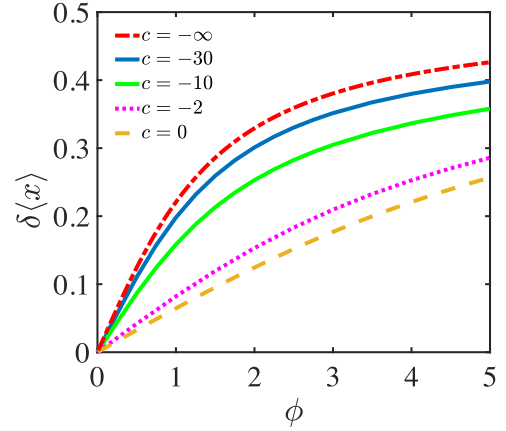

FIG. 3. NHSE in attractive interacting bosons for the bound state. The deviation of mean position $\delta\langle x \rangle$ (in units of L) as a function of ϕ for different interaction strengths from noninteracting (dashed line) to infinite attractive limit (dot-dashed line). ϕ and c are in units of $1/L$. Here we choose $L = 1$ as length unit and set $N = 4$.

IV. NHSE IN ATTRACTIVE INTERACTION

Section III deals with the situation of repulsive interaction. We now turn to study the NHSE in attractive interaction. What should be pointed out is that unlike the case of repulsive interaction, the solution of BAEs in attractive interaction is not unique, which contains bound state and scattering states. Physically, there exists a bound state when bosons attract each other, reflected in the complex solution of quasimomenta $\{k_j\}$ in BAEs. In the weak interaction region, the ground-state solution of quasimomenta consists of $N/2$ (N is an even number) pairs of conjugate complex roots, i.e., $N/2$ dimers $k_{2j-1} = \alpha_j - i\beta_j$, $k_{2j} = \alpha_j + i\beta_j$ ($j = 1, \ldots, N/2$). The state made up of $N/2$ dimers is also called $N/2$ two-string. The M-string state is defined by M quasimomenta sharing the same real part but unequal conjugate imaginary parts, which can be labeled as $k_j = \alpha + \beta_j$ ($j = 1, \ldots, M$). According to the bound-state solution of BAEs, as the attractive interaction strength increases, the ground state evolves from a $N/2$ two-string state gradually to an intermediate state characterized by an M-string ($N > M > 2$) plus $(N - M)/2$ two-string and finally turns to a N-string state.

The bound-state solution of BAEs shows that the NHSE exists in the entire range of interaction strength $c \leqslant 0$ as shown in Fig. 3. Moreover, the deviation $\delta\langle x \rangle$ tends to increase with the growth of attractive strength. This is because the bosons tend to clump together with increasing attraction among them. We can also understand the NHSE in attractive interaction in terms of quantitative analysis in two limits. For the noninteracting limit, all bosons occupy the single-particle ground state $k_j = \pi/L$ and the corresponding ground-state wave function is simply written as $\Psi(x_1, x_2, \ldots, x_N) = \prod_{j=1}^{N} \sin(j\pi x_j/L) \exp(\phi x_j)$ which produces the deviation of mean position $\delta\langle x \rangle = \frac{L}{2}[\coth(\phi L) - \frac{1}{\phi L} - \frac{2\phi L}{\pi^2 + \phi^2 L^2}]$. In strongly attractive limit $c = -\infty$, the system forms a N-body bound state corresponding to the N-string state. At this point, the quasimomentum distribution is given by $k_j = K/N + i(N + 1 - 2j)c/2$, $(j = 1, 2, \ldots, N)$ where

K signifies the total momentum, which is determined by the following transcendental equation:

$$KL = \pi I + 2 \sum_{j=1}^{N-1} \arctan \frac{jcN}{2K} \qquad (17)$$

with $I = N$ for the ground state. We can see that in the limit of $c \to -\infty$, the total momentum is $K = \pi/L$ which indicates each boson has the real part π/NL in the strong attractive limit and the corresponding ground-state wave function can be written as

$$\Psi(x_1, x_2, \ldots, x_N) = \sin(\pi x/L) \exp(N\phi x), \qquad (18)$$

where $x = \frac{x_1 + x_2 + \cdots + x_N}{N}$ denotes the center-of-mass coordinate. The wave function (18) gives a clear physical picture that the system forms a giant molecule of N bosons involving the movement of the center of mass. And similarly, the deviation of mean position derived from (18) yields

$$\delta \langle x \rangle = \frac{L}{2} \left[\coth \Phi L - \frac{1}{\Phi L} - \frac{2\Phi L}{\pi^2 + \Phi^2 L^2} \right], \qquad (19)$$

with $\Phi = N\phi$. We can see that the $\delta \langle x \rangle$ of infinitely attractive bosons is similar to the one of free bosons in form but contains a factor N. Physically, it comes from the Bose enhancement that all bosons tend to locate at the same position.

Next, we turn to address the case of scattering states on the attractive side. In fact, there are real solutions corresponding to scattering states in BAEs (10) for $c < 0$ although its ground state is a string solution (bound state). In the strong interaction regime, this kind of scattering state is referred to as super-Tonks-Girardeau (STG) gas in the literature [142–146]. For the purpose of analysis, we alternatively rewrite the BAEs (10) as the following logarithm form:

$$k_j L = \pi I_j - \sum_{l=1(\neq j)}^{N} \left(\arctan \frac{k_j - k_l}{|c|} + \arctan \frac{k_j + k_l}{|c|} \right). \qquad (20)$$

Here we choose $I_j = j$, such that the quasimomentum distribution in $c \to -\infty$ determined from Eq. (20) connects to the TG limit from Eq. (11) where $k_j = j\pi/L$ ($j = 1, 2, \ldots, N$). Under this circumstance, one would obtain the deviation of mean position $\delta \langle x \rangle$ as a continuous function of $1/c$ as shown in Fig. 4(a). We can recognize that in contrast to the bound state on the attractive side, the scattering state exhibits a nonmonotonic behavior where $\delta \langle x \rangle$ decreases first and then increases as the attractive strength weakens. And also the transition point [the inset of Fig. 4(a)] locates at the STG regime ($-1 \ll 1/c < 0$). The nonmonotonic behavior is closely related to the density distribution on the attractive side. In the limit of $c \to -\infty$, the density profile is identical to the one in the TG limit displaying N peaks with near equidistance. Then, the density distribution gradually migrates toward boundaries as the attraction decreases, suppressing the NHSE. However, as the attraction is getting weaker, the density tends to concentrate in the center of potential with a larger weight which can magnify the NHSE. Finally, in the weak attraction limit, there emerge $2N - 1$ peaks in the density distribution as shown in Fig. 4(b). This is because the bosons occupy N lowest odd single-particle orbitals $k_j = (2j + 1)\pi/L$ when $c \to 0^-$.
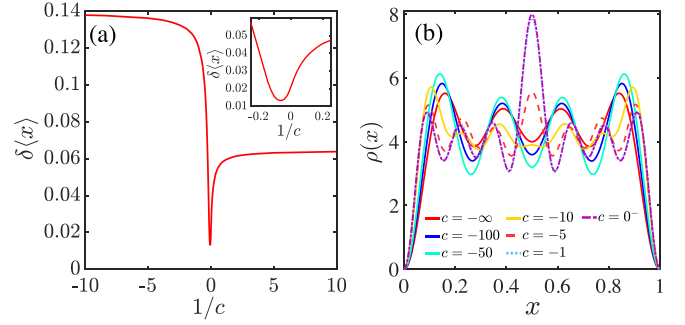

FIG. 4. (a) The deviation of mean position $\delta \langle x \rangle$ (in units of L) as a function of inverse interaction strength at $\phi = 1$ for the scattering state. (b) Density distributions of the scattering state for different attractive interaction strengths from noninteracting (dashed line) to infinite attractive limit (dot-dashed line). ϕ and c are in units of $1/L$. Here we choose $L = 1$ as length unit and set $N = 4$.

V. SUMMARY AND OUTLOOK

In summary, through the example of non-Hermitian 1D interacting Bose gas, we investigated the NHSE in a non-Hermitian many-body system. Utilizing the Bethe ansatz, we obtained the exact solutions, including quasimomenta, eigenenergies, and wave functions of the system in OBC. The NHSE can be characterized by density distribution and momentum distribution. Our calculations show that the NHSE exists in the entire interaction regime and displays distinct responses to the interaction effect. The main conclusions are summarized as follows.

(i) For repulsive interaction $c > 0$, the NHSE is gradually suppressed as interaction strength increases but does not vanish even in the TG limit ($c \to +\infty$).

(ii) For the bound state in attractive interaction $c < 0$, the system consists of N bosons from the two-string state into the N-string state as the attractive interaction strength grows. And in this process, the NHSE is enhanced.

(iii) For the scattering state in attractive interaction $c < 0$, we find a nonmonotonic behavior in the deviation of mean position $\delta \langle x \rangle$ where the NHSE is first suppressed and then enhanced while interaction weakens.

Our non-Hermitian many-body model can, in principle, be realized in current cold atom experiments, which offers an ideal platform to observe the NHSE. Thanks to the flexible tunability, cold atomic gases have realized the tunable nonreciprocal model (with unequal hopping strength) through a dissipative Aharonov-Bohm ring [131] and observed dynamic signatures of the NHSE [107]. Our non-Hermitian Lieb-Liniger model describes the low-filling regime of the 1D Bose-Hubbard mode, which could be realized from the aforementioned nonreciprocal model by adding tunable interactions. The NHSE in continuum space is proposed to be observed via dynamic measurements [94]. In situations with and without NHSE, respectively, a right-moving wave package will either be localized near the right boundary after touching it, or reflected as in the usual cases. We believe our model can also be realized in a similar way by adding proper interactions.

This paper provides some preliminary exploration of the NHSE in many-body systems from the view of exactly

solvable many-body models. Our results build on the rapidly expanding field of non-Hermitian physics. Considerably more work will be desired to explore the interplay between the NHSE and other kinds of exactly solvable many-body systems and further accomplish more comprehensive investigations for future research.

APPENDIX A: SINGLE-PARTICLE NON-HERMITIAN SKIN EFFECT IN THE TIGHT-BINDING MODEL

In this Appendix we give a brief introduction to the non-Hermitian skin effect at a single-particle level. We consider a one-dimensional tight-binding model with unequal hopping, whose Hamiltonian is written as

$$\hat{H} = t_1 \sum_n |n+1\rangle\langle n| + t_2 \sum_n |n\rangle\langle n+1|, \quad \text{(A1)}$$

where $t_1 > t_2$ denote the unequal hopping amplitudes. This non-Hermitian model with disorder potential was first introduced by Hatano and Nelson [147] to investigate localization transition and is investigated in ultracold atoms [148,149]. Now we solve its eigenvalues and eigenvectors. Under PBC, the momentum is a good quantum number ($k = 0, 2\pi/L, \ldots, 2\pi(L-1)/L$). Then the eigenenergies and eigenstates are given by

$$E_k = t_1 e^{-ik} + t_2 e^{ik}, \quad |E_k\rangle = \frac{1}{\sqrt{L}} \sum_n e^{ikn} |n\rangle, \quad \text{(A2)}$$

from which we can see the eigenvector is nothing but the Bloch state which is identical to the Hermitian case but the spectrum becomes complex.

Under OBC, the momentum is not a good quantum number anymore. Expanding the eigenvector in real space $|E\rangle = \sum_n \psi_n |n\rangle$, we have

$$E\psi_n = t_1 \psi_{n-1} + t_2 \psi_{n+1}, \quad \text{(A3)}$$

with OBC $\psi_0 = \psi_{L+1} = 0$. We introduce a non-Bloch wave function $\psi_n = A_1 \beta_1^n + A_2 \beta_2^n$, and then the eigenvalues are determined by

$$E(\beta) = t_1/\beta_a + t_2\beta_a, \quad \text{(A4)}$$

where $a = 1, 2$. The boundary conditions $\psi_0 = 0$ and $\psi_{L+1} = 0$ give

$$A_1 + A_2 = 0, \quad A_1\beta_1^{L+1} + A_2\beta_2^{L+1} = 0, \quad \text{(A5)}$$

which will lead to the condition $\beta_1^{L+1} = \beta_2^{L+1}$. Together with $\beta_1\beta_2 = t_1/t_2$, we can obtain

$$\beta_1 = \sqrt{t_1/t_2}\, e^{i\theta_m} = \beta_2^*, \quad \theta_m = \pi m/(L+1), \quad \text{(A6)}$$

with $m = 1, 2, \ldots, L$. Therefore, we can derive the eigenenergies in OBC

$$E_m = 2\sqrt{t_1 t_2} \cos\theta_m, \quad \text{(A7)}$$

and associated eigenstates

$$|E_m\rangle = \sum_n e^{n\phi} \sin n\theta_m |n\rangle, \quad \text{(A8)}$$

where $\phi = \ln\sqrt{t_1/t_2}$ denotes the strength of the imaginary potential. Note that the spectrum in OBC is always real. This is because the Hamiltonian at OBC can be mapped to a Hermitian counterpart via a gauge transformation $|n\rangle \rightarrow e^{-n\phi}|n\rangle$, $\langle n| \rightarrow \langle n|e^{\phi}$. The spectrum is determined by the Hermitian counterpart. Meanwhile, the non-Bloch wave function consists of the standing wave $\sin(n\theta_m)$ with an amplification factor $e^{n\phi}$ exhibiting exponential accumulation at the boundary. This feature is called the non-Hermitian skin effect. The non-Bloch wave function in the eigenstate (A8) will be the starting point for solving non-Hermitian many-body systems.

APPENDIX B: PHYSICAL REALIZATION OF THE NONRECIPROCAL MODEL LATTICE MODEL

This Appendix discusses the experimental realization of the tight-binding model with unequal hopping discussed in Appendix A on a cold atom setup [131]. The imaginary potential in the main text is related to the local loss rate induced by reservoirs. To elaborately explain it, we tackle the procedure in two steps. The first is to derive the local loss rate from the coupling between the system and reservoir. The second is to discuss how the local loss rate induces unequal hopping between the nearest-neighbor site. We start from a lattice system as illustrated in Fig. 5(a), where a three-site triangle ring couples a reservoir. The total Hamiltonian is given by

$$\hat{H}_{\text{ring}} = \sum_{n<-2} t_r(\hat{a}_n^\dagger \hat{a}_{n+1} + \text{H.c.}) + t_c(\hat{a}_{-2}^\dagger \hat{a}_{-1} + \text{H.c.})$$
$$+ (t'e^{i\Phi/2}\hat{a}_{-1}^\dagger \hat{a}_0 + t\hat{a}_1^\dagger \hat{a}_0 + t'e^{i\Phi/2}\hat{a}_1^\dagger \hat{a}_{-1} + \text{H.c.}). \quad \text{(B1)}$$

The first term is the bulk Hamiltonian of the reservoir, the last term denotes the triangle part, and the second term is the coupling between them with coupling strength t_c. The phase Φ sets up a synthetic magnetic flux in the ring, and the hopping strengths t_r, t_c, t', and t can be tuned independently by laser beams.

Integrating the reservoir degree of freedoms ($n < -1$), one can derive the following Hamiltonian ($t_c \ll t_r$):

$$\hat{H}_{\text{loss}} = -i\Gamma\hat{a}_{-1}^\dagger \hat{a}_{-1} + (t'\hat{a}_0^\dagger \hat{a}_{-1} + t\hat{a}_1^\dagger \hat{a}_0 + t'e^{i\Phi}\hat{a}_1^\dagger \hat{a}_{-1} + \text{H.c.}), \quad \text{(B2)}$$

where $\Gamma = t_c^2/t_r$ is the effective loss rate induced by the reservoir which can be derived from Fermi's "golden rule." Based on the local loss model $\hat{H}_{\text{loss}}$, next we derive the 1D tight-binding model with unequal hopping as studied in Appendix A. Consider a 1D tight-binding chain with hopping t hybridizing local impurities with amplitude t' and phase $\Phi/2$
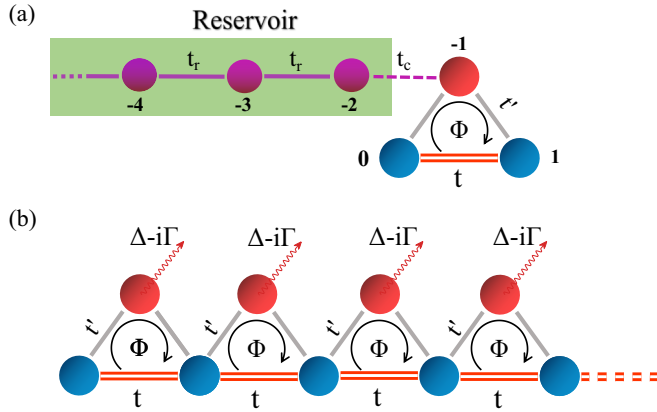
FIG. 5. (a) Schematic diagram of a three-site ring system coupled to a reservoir (shaded area). The reservoir consists of a 1D tight-binding chain with hopping strength t_r in bulk and t_c (dashed line) between the reservoir and one site in the system (red circle). Hopping amplitudes inside the system are denoted by t' (gray bond) and t (double red bond), respectively. There is a synthetic magnetic flux Φ inside the system, which is implemented by the phase of hopping term t' [see Eq. (B1)]. (b) Schematic of the 1D tight-binding chain with local loss which effectively produces a nonreciprocal model with unequal hopping exhibiting the NHSE. Here Δ and Γ represent the energy offset and loss rate, respectively.

as shown in Fig. 5(b). The corresponding Hamiltonian reads

$$\hat{H}_{\text{chain}} = (\Delta - i\Gamma) \sum_j \hat{d}_j^\dagger \hat{d}_j + t \sum_n (\hat{a}_n^\dagger \hat{a}_{n+1} + \text{H.c.})$$
$$+ \sum_n \left[t' e^{i\frac{\Phi}{2}} \hat{d}_n^\dagger \hat{a}_n + t' e^{i\frac{\Phi}{2}} \hat{a}_{n+1}^\dagger \hat{d}_n + \text{H.c.} \right], \quad \text{(B3)}$$

where Γ denotes the local loss rate, and Δ is the on-site energy offset. The first term is the local impurity part with on-site loss. The second term denotes the system part, and the third represents the hybridization between the system and impurities. For convenience, we fix the phase as $\Phi = \pi/2$ for a concrete experimental setup. In the weak-coupling regime $t' \ll \sqrt{\Delta^2 + \Gamma^2}$, one can eliminate impurity degrees of freedom and derive the following effective Hamiltonian utilizing second-order perturbation theory:

$$\hat{H}_{\text{eff}} = \sum_n [(t+\gamma)\hat{a}_{n+1}^\dagger \hat{a}_n + (t-\gamma)\hat{a}_n^\dagger \hat{a}_{n+1}], \quad \text{(B4)}$$

where $\gamma = \frac{(i\Delta - \Gamma)t'^2}{\Delta^2 + \Gamma^2}$. The unequal hopping originates from the second-order process that a particle hops from the the nth site to the nth impurity and then to the $(n+1)$th site, accompanied by a phase factor. One can find that the imaginary potential introduced in Appendix A or in the non-Hermitian Hamiltonian (1) is determined by the local loss rate via $\phi = \ln \frac{|t+\gamma|}{|t-\gamma|}$. Here we have ignored the single site term $\hat{a}_n^\dagger \hat{a}_n$ which is irrelevant to the NHSE. It is worth emphasizing that while the Hamiltonian (B4) is derived through perturbation theory within the parameter condition $t' \ll \sqrt{\Delta^2 + \gamma^2}$, the NHSE exists far beyond the perturbative condition [131]. Another important issue is that the lattice model is generally not exactly solvable when interaction [e.g., the on-site term $U\hat{n}_j(\hat{n}_j - 1)$] is introduced, but the interaction does not destroy the NHSE. The nonintegrable many-body lattice models supporting the NHSE are worth further investigation in the future.

[1] G. Gamow, Z. Phys. **51**, 204 (1928).
[2] R. J. Mason and M. Tabak, Phys. Rev. Lett. **80**, 524 (1998).
[3] E. J. Bergholtz, J. C. Budich, and F. K. Kunst, Rev. Mod. Phys. **93**, 015005 (2021).
[4] Y. Ashida, Z. Gong, and M. Ueda, Adv. Phys. **69**, 249 (2020).
[5] G. Barontini, R. Labouvie, F. Stubenrauch, A. Vogler, V. Guarrera, and H. Ott, Phys. Rev. Lett. **110**, 035302 (2013).
[6] Y. S. Patil, S. Chakram, and M. Vengalattore, Phys. Rev. Lett. **115**, 140402 (2015).
[7] R. Labouvie, B. Santra, S. Heun, and H. Ott, Phys. Rev. Lett. **116**, 235302 (2016).
[8] H. P. Lüschen, P. Bordia, S. S. Hodgman, M. Schreiber, S. Sarkar, A. J. Daley, M. H. Fischer, E. Altman, I. Bloch, and U. Schneider, Phys. Rev. X **7**, 011034 (2017).
[9] T. Tomita, S. Nakajima, Y. Takasu, and Y. Takahashi, Phys. Rev. A **99**, 031601(R) (2019).
[10] R. Bouganne, M. B. Aguilera, A. Ghermaoui, and F. Gerbier, Nat. Phys. **16**, 21 (2020).
[11] T. Tomita, S. Nakajima, I. Danshita, Y. Takasu, and Y. Takahashi, Sci. Adv. **3**, e1701513 (2017).
[12] K. Sponselee, L. Freystatzky, B. Abeln, M. Diem, B. Hundt, A. Kochanke, T. Ponath, B. Santra, L. Mathey, K. Sengstock, and C. Becker, Quantum Sci. Technol. **4**, 014002 (2018).
[13] Y. Takasu, T. Yagami, Y. Ashida, R. Hamazaki, Y. Kuno, and Y. Takahashi, Prog. Theor. Exp. Phys. **2020**, 12A110 (2020).
[14] B. Yan, S. A. Moses, B. Gadway, J. P. Covey, K. R. Hazzard, A. M. Rey, D. S. Jin, and J. Ye, Nature (London) **501**, 521 (2013).
[15] F. Schäfer, T. Fukuhara, S. Sugawa, Y. Takasu, and Y. Takahashi, Nat. Rev. Phys. **2**, 411 (2020).
[16] K. Kawabata, Y. Ashida, and M. Ueda, Phys. Rev. Lett. **119**, 190401 (2017).
[17] Y. Ashida, S. Furukawa, and M. Ueda, Nat. Commun. **8**, 15791 (2017).
[18] L. Pan, S. Chen, and X. Cui, Phys. Rev. A **99**, 011601(R) (2019).
[19] L. Pan, S. Chen, and X. Cui, Phys. Rev. A **99**, 063616 (2019).
[20] Z. Zhou and Z. Yu, Phys. Rev. A **99**, 043412 (2019).
[21] K. Yamamoto, M. Nakagawa, K. Adachi, K. Takasan, M. Ueda, and N. Kawakami, Phys. Rev. Lett. **123**, 123601 (2019).
[22] N. Okuma and M. Sato, Phys. Rev. Lett. **123**, 097701 (2019).
[23] L. Zhou and X. Cui, iScience **14**, 257 (2019).
[24] L. Pan, X. Chen, Y. Chen, and H. Zhai, Nat. Phys. **16**, 767 (2020).
[25] T. Yoshida, K. Kudo, and Y. Hatsugai, Sci. Rep. **9**, 16895 (2019).

[26] T. Liu, J. J. He, T. Yoshida, Z.-L. Xiang, and F. Nori, Phys. Rev. B **102**, 235151 (2020).

[27] Z. H. Xu and S. Chen, Phys. Rev. B **102**, 035153 (2020).

[28] K. Kawabata, K. Shiozaki, and S. Ryu, Phys. Rev. B **105**, 165137 (2022).

[29] S.-B. Zhang, M. M. Denner, T. Bzdušek, M. A. Sentef, and T. Neupert, Phys. Rev. B **106**, L121102 (2022).

[30] F. Alsallom, L. Herviou, O. V. Yazyev, and M. Brzezińska, arXiv:2110.13164.

[31] J. Carlström, Phys. Rev. Res. **2**, 013078 (2020).

[32] Z. Cai and T. Barthel, Phys. Rev. Lett. **111**, 150403 (2013).

[33] T.-S. Deng, L. Pan, Y. Chen, and H. Zhai, Phys. Rev. Lett. **127**, 086801 (2021).

[34] Z. Wang, Q. Li, W. Li, and Z. Cai, Phys. Rev. Lett. **126**, 237201 (2021).

[35] T.-S. Deng and L. Pan, Phys. Rev. B **104**, 094306 (2021).

[36] B. Buča, C. Booker, M. Medenjak, and D. Jaksch, New J. Phys. **22**, 123040 (2020).

[37] K. Yamamoto, Y. Ashida, and N. Kawakami, Phys. Rev. Res. **2**, 043343 (2020).

[38] K. Yamamoto, M. Nakagawa, N. Tsuji, M. Ueda, and N. Kawakami, Phys. Rev. Lett. **127**, 055301 (2021).

[39] R. Hanai, A. Edelman, Y. Ohashi, and P. B. Littlewood, Phys. Rev. Lett. **122**, 185301 (2019).

[40] K. L. Zhang and Z. Song, Phys. Rev. Lett. **126**, 116401 (2021).

[41] X. Z. Zhang and Z. Song, Phys. Rev. B **104**, 094301 (2021).

[42] X. Z. Zhang, L. Jin, and Z. Song, Phys. Rev. B **101**, 224301 (2020).

[43] K. L. Zhang and Z. Song, Phys. Rev. B **104**, 245140 (2021).

[44] D. Sticlet, B. Dóra, and C. P. Moca, Phys. Rev. Lett. **128**, 016802 (2022).

[45] B. Dóra and C. P. Moca, Phys. Rev. Lett. **124**, 136802 (2020).

[46] Á. Bácsi, C. P. Moca, and B. Dóra, Phys. Rev. Lett. **124**, 136401 (2020).

[47] J.-S. Bernier, R. Tan, C. Guo, C. Kollath, and D. Poletti, Phys. Rev. B **102**, 115156 (2020).

[48] L. Pan, X. Wang, X. Cui, and S. Chen, Phys. Rev. A **102**, 023306 (2020).

[49] X. Z. Zhang and Z. Song, Phys. Rev. B **102**, 174303 (2020).

[50] X. Z. Zhang and Z. Song, Phys. Rev. B **103**, 235153 (2021).

[51] T. Hayata and A. Yamamoto, Phys. Rev. B **104**, 125102 (2021).

[52] K. Yang, S. C. Morampudi, and E. J. Bergholtz, Phys. Rev. Lett. **126**, 077201 (2021).

[53] X. Cui, Phys. Rev. Res. **4**, 013047 (2022).

[54] M. Nakagawa, N. Kawakami, and M. Ueda, Phys. Rev. Lett. **126**, 110404 (2021).

[55] M. Nakagawa, N. Tsuji, N. Kawakami, and M. Ueda, Phys. Rev. Lett. **124**, 147203 (2020).

[56] R. Hamazaki, K. Kawabata, and M. Ueda, Phys. Rev. Lett. **123**, 090603 (2019).

[57] L.-J. Zhai, S. Yin, and G.-Y. Huang, Phys. Rev. B **102**, 064206 (2020).

[58] K. Suthar, Y.-C. Wang, Y.-P. Huang, H.-H. Jen, and J.-S. You, Phys. Rev. B **106**, 064208 (2022).

[59] N. Matsumoto, K. Kawabata, Y. Ashida, S. Furukawa, and M. Ueda, Phys. Rev. Lett. **125**, 260601 (2020).

[60] S. Sarkar, Sci. Rep. **11**, 5510 (2021).

[61] M. Nakagawa, N. Kawakami, and M. Ueda, Phys. Rev. Lett. **121**, 203001 (2018).

[62] J. A. S. Lourenço, R. L. Eneias, and R. G. Pereira, Phys. Rev. B **98**, 085126 (2018).

[63] R. Hanai and P. B. Littlewood, Phys. Rev. Res. **2**, 033018 (2020).

[64] K. Yamamoto, M. Nakagawa, M. Tezuka, M. Ueda, and N. Kawakami, Phys. Rev. B **105**, 205125 (2022).

[65] Y.-N. Zhou, L. Mao, and H. Zhai, Phys. Rev. Res. **3**, 043060 (2021).

[66] P. Zhang, S.-K. Jian, C. Liu, and X. Chen, Quantum **5**, 579 (2021).

[67] L. Sá, P. Ribeiro, and T. Prosen, Phys. Rev. X **10**, 021019 (2020).

[68] J. Li, T. Prosen, and A. Chan, Phys. Rev. Lett. **127**, 170602 (2021).

[69] G. Sun, J.-C. Tang, and S.-P. Kou, Front. Phys. **17**, 33502 (2022).

[70] S. Mu, C. H. Lee, L. Li, and J. Gong, Phys. Rev. B **102**, 081115(R) (2020).

[71] F. Qin, R. Shen, and C. H. Lee, Phys. Rev. A **107**, L010202 (2023).

[72] S. Yao and Z. Wang, Phys. Rev. Lett. **121**, 086803 (2018).

[73] S. Yao, F. Song, and Z. Wang, Phys. Rev. Lett. **121**, 136802 (2018).

[74] F. K. Kunst, E. Edvardsson, Jan C. Budich, and E. J. Bergholtz, Phys. Rev. Lett. **121**, 026808 (2018).

[75] F. Song, S. Yao, and Z. Wang, Phys. Rev. Lett. **123**, 170401 (2019).

[76] F. Song, S. Yao, and Z. Wang, Phys. Rev. Lett. **123**, 246801 (2019).

[77] H. Jiang, L.-J. Lang, C. Yang, S.-L. Zhu, and S. Chen, Phys. Rev. B **100**, 054301 (2019).

[78] C.-X. Guo, C.-H. Liu, X.-M. Zhao, Y. Liu, and S. Chen, Phys. Rev. Lett. **127**, 116801 (2021).

[79] L. Jin and Z. Song, Phys. Rev. B **99**, 081103(R) (2019).

[80] D. S. Borgnia, A. J. Kruchkov, and R.-J. Slager, Phys. Rev. Lett. **124**, 056802 (2020).

[81] S. Longhi, Phys. Rev. Res. **1**, 023013 (2019).

[82] K. Zhang, Z. Yang, and C. Fang, Phys. Rev. Lett. **125**, 126402 (2020).

[83] C. H. Lee, L. Li, and J. Gong, Phys. Rev. Lett. **123**, 016805 (2019).

[84] L. Li, C. H. Lee, and J. Gong, Phys. Rev. Lett. **124**, 250402 (2020).

[85] L. Li, C. H. Lee, S. Mu, and J. Gong, Nat. Commun. **11**, 5491 (2020).

[86] C.-H. Liu, K. Zhang, Z. Yang, and S. Chen, Phys. Rev. Res. **2**, 043167 (2020).

[87] J. C. Budich and E. J. Bergholtz, Phys. Rev. Lett. **125**, 180403 (2020).

[88] Z. Yang, K. Zhang, C. Fang, and J. Hu, Phys. Rev. Lett. **125**, 226402 (2020).

[89] T. Yoshida, T. Mizoguchi, and Y. Hatsugai, Phys. Rev. Res. **2**, 022062(R) (2020).

[90] Y. Yi and Z. Yang, Phys. Rev. Lett. **125**, 186802 (2020).

[91] N. Okuma, K. Kawabata, K. Shiozaki, and M. Sato, Phys. Rev. Lett. **124**, 086801 (2020).

[92] S. Longhi, Phys. Rev. Lett. **124**, 066602 (2020).

[93] Z. Zhou and Z. Yu, Phys. Rev. A **106**, 032216 (2022).

[94] S. Guo, C. Dong, F. Zhang, J. Hu, and Z. Yang, Phys. Rev. A **106**, L061302 (2022).

[95] L. Zhou, H. Li, W. Yi, and X. Cui, Commun. Phys. **5**, 252 (2022).

[96] K. Zhang, Z. Yang, and C. Fang, Nat. Commun. **13**, 2496 (2022).

[97] Y. Peng, J. Jie, D. Yu, and Y. Wang, Phys. Rev. B **106**, L161402 (2022).

[98] X. Zhang, T. Zhang, M.-H. Lu, and Y.-F. Chen, arXiv:2205.08037.

[99] T. Helbig, T. Hofmann, S. Imhof, M. Abdelghany, T. Kiessling, L. W. Molenkamp, C. H. Lee, A. Szameit, M. Greiter, and R. Thomale, Nat. Phys. **16**, 747 (2020).

[100] T. Hofmann, T. Helbig, F. Schindler, N. Salgo, M. Brzezinska, M. Greiter, T. Kiessling, D. Wolf, A. Vollhardt, A. Kabasi, C. H. Lee, A. Bilusic, R. Thomale, and T. Neupert, Phys. Rev. Res. **2**, 023265 (2020).

[101] L. Xiao, T. Deng, K. Wang, G. Zhu, Z. Wang, W. Yi, and P. Xue, Nat. Phys. **16**, 761 (2020).

[102] A. Ghatak, M. Brandenbourger, J. van Wezel, and C. Coulais, Proc. Natl. Acad. Sci. USA **117**, 29561 (2020).

[103] S. Weidemann, M. Kremer, T. Helbig, T. Hofmann, A. Stegmaier, M. Greiter, R. Thomale, and A. Szameit, Science **368**, 311 (2020).

[104] D. Zou, T. Chen, W. He, J. Bao, C. H. Lee, H. Sun, and X. Zhang, Nat. Commun. **12**, 7201 (2021).

[105] L. Zhang, Y. Yang, Y. Ge, Y.-J. Guan, Q. Chen, Q. Yan, F. Chen, R. Xi, Y. Li, D. Jia, S.-Q. Yuan, H.-X. Sun, H. Chen, and B. Zhang, Nat. Commun. **12**, 6297 (2021).

[106] X. Zhang, Y. Tian, J.-H. Jiang, M.-H. Lu, and Y.-F. Chen, Nat. Commun. **12**, 5377 (2021).

[107] Q. Liang, D. Xie, Z. Dong, H. Li, H. Li, B. Gadway, W. Yi, and B. Yan, Phys. Rev. Lett. **129**, 070401 (2022).

[108] C. H. Lee, Phys. Rev. B **104**, 195102 (2021).

[109] R. Shen and C. H. Lee, arXiv:2107.03414.

[110] D.-W. Zhang, Y.-L. Chen, G.-Q. Zhang, L.-J. Lang, Z. Li, and S.-L. Zhu, Phys. Rev. B **101**, 235150 (2020).

[111] Z. Wang, L.-J. Lang, and L. He, Phys. Rev. B **105**, 054315 (2022).

[112] N. Okuma and M. Sato, Phys. Rev. Lett. **126**, 176601 (2021).

[113] Y.-N. Wang, W.-L. You, and G. Sun, Phys. Rev. A **106**, 053315 (2022).

[114] E. H. Lieb and W. Liniger, Phys. Rev. **130**, 1605 (1963).

[115] N. Andrei, K. Furuya, and J. H. Lowenstein, Rev. Mod. Phys. **55**, 331 (1983).

[116] M. V. Medvedyeva, F. H. L. Essler, and T. Prosen, Phys. Rev. Lett. **117**, 137202 (2016).

[117] G. Akemann, M. Kieburg, A. Mielke, and T. Prosen, Phys. Rev. Lett. **123**, 254101 (2019).

[118] F. H. L. Essler and L. Piroli, Phys. Rev. E **102**, 062210 (2020).

[119] A. A. Ziolkowska and F. Essler, SciPost Phys. **8**, 044 (2020).

[120] M. de Leeuw, C. Paletta, and B. Pozsgay, Phys. Rev. Lett. **126**, 240403 (2021).

[121] V. Popkov and C. Presilla, Phys. Rev. Lett. **126**, 190402 (2021).

[122] P. W. Claeys and A. Lamacraft, Phys. Rev. Res. **4**, 013033 (2022).

[123] L. Su and I. Martin, Phys. Rev. B **106**, 134312 (2022).

[124] C. P. Moca, M. A. Werner, Ö. Legeza, T. Prosen, M. Kormos, and G. Zaránd, Phys. Rev. B **105**, 195144 (2022).

[125] L. Sá, P. Ribeiro, and T. Prosen, Phys. Rev. Res. **4**, L022068 (2022).

[126] T. Kinoshita, T. Wenger, and D. S. Weiss, Science **305**, 1125 (2004).

[127] B. Paredes, A. Widera, V. Murg, O. Mandel, S. Fölling, I. Cirac, G. V. Shlyapnikov, T. W. Hänsch, and I. Bloch, Nature (London) **429**, 277 (2004).

[128] T. Kinoshita, T. Wenger, and D. S. Weiss, Phys. Rev. Lett. **95**, 190406 (2005).

[129] M. Olshanii, Phys. Rev. Lett. **81**, 938 (1998).

[130] C. Chin, R. Grimm, P. Julienne, and E. Tiesinga, Rev. Mod. Phys. **82**, 1225 (2010).

[131] W. Gou, T. Chen, D. Xie, T. Xiao, T.-S. Deng, B. Gadway, W. Yi, and B. Yan, Phys. Rev. Lett. **124**, 070402 (2020).

[132] S. Dürr, J. J. García-Ripoll, N. Syassen, D. M. Bauer, M. Lettner, J. I. Cirac, and G. Rempe, Phys. Rev. A **79**, 023614 (2009).

[133] J. J. García-Ripoll, S. Dürr, N. Syassen, D. M. Bauer, M. Lettner, G. Rempe, and J. I. Cirac, New J. Phys. **11**, 013053 (2009).

[134] M. Kiffner and M. J. Hartmann, New J. Phys. **13**, 053027 (2011).

[135] I. Bouchoule, B. Doyon, and J. Dubail, SciPost Phys. **9**, 044 (2020).

[136] I. Bouchoule and J. Dubail, Phys. Rev. Lett. **126**, 160603 (2021).

[137] L. Rosso, A. Biella, and L. Mazza, SciPost Phys. **12**, 044 (2022).

[138] M. T. Batchelor, X. W. Guan, N. Oelkers, and C. Lee, J. Phys. A: Math. Gen. **38**, 7787 (2005).

[139] N. Oelkers, M. T. Batchelor, M. Bortz, and X. W. Guan, J. Phys. A: Math. Gen. **39**, 1073 (2006).

[140] A. del Campo and J. G. Muga, Europhys. Lett. **74**, 965 (2006).

[141] Y. Hao, Y. Zhang, J. Q. Liang, and S. Chen, Phys. Rev. A **73**, 063617 (2006).

[142] G. E. Astrakharchik, J. Boronat, J. Casulleras, and S. Giorgini, Phys. Rev. Lett. **95**, 190407 (2005).

[143] M. T. Batchelor, M. Bortz, X. W. Guan, and N. Oelkers, J. Stat. Mech. (2005) L10001.

[144] S. Chen, L. Guan, X. Yin, Y. Hao, and X.-W. Guan, Phys. Rev. A **81**, 031609(R) (2010).

[145] M. Panfil, J. De Nardis, and J.-S. Caux, Phys. Rev. Lett. **110**, 125302 (2013).

[146] M. Kormos, G. Mussardo, and A. Trombettoni, Phys. Rev. A **83**, 013617 (2011).

[147] N. Hatano and D. R. Nelson, Phys. Rev. Lett. **77**, 570 (1996).

[148] K. Li and Y. Xu, Phys. Rev. Lett. **129**, 093001 (2022).

[149] C. Lv, R. Zhang, Z. Zhai, and Q. Zhou, Nat. Commun. **13**, 2184 (2022).